

Wide Band Low RCS Metasurface and Its Application on Patch Antenna

Kavitha Muthukrishnan* and Venkateswaran Narasimhan

Abstract—A new metasurface (MS) structure for wideband low radar cross section (RCS) and its performance as an antenna has been analyzed and proposed in this paper. The MS has been designed with two different AMC unit cells, and the novel AMCs scatter the incident waves diffusively. The parameters and dimensions of the AMCs are optimized to get the best performance of the antenna. Furthermore, the unit cell structure of metasurface is designed and positioned to improve the directivity of the antenna. The reflected electromagnetic waves scatter in a manner of 180° out of phase with the incident waves, and the antenna's scattering and radiation performance has also been examined. Full-wave simulations and measurements confirm that the proposed antenna achieves 10 dB RCS reduction over a wide bandwidth of 3–12 GHz (61.2%). A monostatic peak RCS reduction of 45 dB is accomplished at 5 GHz, 7 GHz, and 11.5 GHz. Besides, the radiation characteristics of the antenna are appropriate in the boresight direction, and the antenna exhibits good performance in E -, H -planes and ensures adequate directivity.

1. INTRODUCTION

Patch antenna designs are widely used in many applications. However, they possess drawbacks such as having low gain and operating in narrow band [1]. Defense applications have inspired researchers to design antennas as a way to reduce the radar cross section (RCS) [2]. Less visibility of an antenna from the radar is an essential feature in stealth platforms, airborne vehicles, and military applications. Thus, low radar signature of an antenna is inherent in the stealthy aircrafts [3]. The Stealth or RCS reduction and control concepts have been the topics of interest for a few decades [4]. Stealth technology lessens the visibility of a target to be detected by radar. With the improvement of modern stealth technology, RCS reduction has received more attention, especially for military platforms. For instance, a stealth platform must have design features to provide low RCS. For such low RCS platforms, antennas are designed to serve as effective radiators and main contributors of total RCS.

The RCS of a traditional antenna can be very large making it an easy target to pick up on basic radar systems. If such an antenna is placed on a stealthy platform, it will destroy the low RCS properties. Thus, the research on RCS reduction for antennas is meaningful [5].

Metamaterials are gaining huge popularity since they are artificially designed to possess a few electromagnetic properties that are not found naturally [6–10]. A left-handed metasurface based travelling wave antenna was introduced in [11]. The aim was to improve the gain and radiation pattern without affecting the fractional bandwidth. In [12], an ultra-wide band miniature integrated antenna was designed using CRLH targeted for transmission lines application. In this design, rectangular and spiral inductors were used. A leaky wave antenna design was proposed in [13]. This design was done using a substrate integrated waveguide model to make it appropriate for applications such as millimeter-wave type beam forming.

Received 10 September 2020, Accepted 21 October 2020, Scheduled 4 November 2020

* Corresponding author: Kavitha Muthukrishnan (kavithasorna@yahoo.com).

The authors are with the Department of ECE, Sri Siva Subramaniya Nadar College of Engineering, Chennai 603110, India.

In recent years, many novel techniques have been proposed to RCS reduction of antennas, such as antenna shaping, using radar absorbing materials (RAM), and using Self-interference cancellation techniques [14–16]. Antenna shaping is one method for RCS reduction. Despite this technique, RCS can be reduced only by decrementing the performance of the antenna. However, the utilization of RAMs for RCS reduction of antenna usually requires a trade-off between radiation characteristics of antennas varying the structures of the original antennas. The other way is the utilization of RAMs. For in-band frequencies, it is tough to decrease the RCS using RAMs because they scatter the energy in specular direction and thus affect the RCS reduction. Another way to RCS reduction of antennas is the use of Frequency Selective Surface (FSS) radomes [17–19]. In this case, the FSS is translucent to electromagnetic waves in the operating band of antennas, while the signal outside the operating band is reflected. However, to obtain favorable RCS reduction, a complex conformal shape should be designed which increases the complexity, weight, and costs.

In [20], reduction of RCS is carried out through in-band and out-band for a Circularly Polarized antenna with corner truncated design. Furthermore, artificial magnetic conductors (AMC) are broadly applied to reduce RCS [21]. Although the patch antenna built with EBG structures minimizes the RCS, the directivity of the antenna is less [22]. Besides, the RCS of antennas can be minimized by utilizing a fractal structure [23] modifying the antenna structure [24]. A dual band metamaterial absorber was utilized to obtain RCSR [25]. Metasurface and its application on a patch antenna has been employed to achieve RCSR [26]. A patch antenna with AMC metasurface eliminates specular scattering of waves from the surface of the antenna [27]. Tan et al. proposed a low RCS, high-gain left handed circularly polarized metasurface antenna (LCP-MA), though their RCSR bandwidth was limited [28]. A wideband small-footprint circularly polarized Fabry-Perot resonator antenna was presented in this paper and had a peak RCSR of 11 dB only [29]. EBG absorbers using conducting polymers were used to achieve RCSR [31]. FSS absorbing ground plane structures were implemented to obtain RCSR, and they have not acquired apparent RCSR [32, 33]. In this paper, the novel AMCs embedded on a planar antenna is proposed, and its effect on wideband RCS reduction is presented. The proposed antenna exhibits enhanced radiation and 10 dB wideband RCS reduction of 3–12 GHz. The dissimilar AMC unit cell arrangement eliminates the specular reflection from the surface, and the wave scatters in unconventional direction. Moreover, the antenna’s radiation performance is also adequate.

The paper is organized as follows. Section 2 gives a detailed description about design and analysis and of the proposed antenna, and Section 3 discusses simulated results. Section 4 illustrates the experiment results obtained in the present work. Subsequently, Section 5 presents the conclusion of the proposed work.

2. DESIGN AND ANALYSIS OF REFERENCE AND AMC BASED METASURFACE ANTENNA

The proposed design of antenna employs a lossy dielectric FR4 substrate. The design combines three layers, slotted patch antenna, AMC1, and AMC2. The parameters of the AMCs are optimized in this design to maximize the performance of the antenna. The proposed unit cell structure has impact in improving the directivity of the antenna. The reflection phase of the metasurface antenna is able to show a shift from $+180^\circ$ to -180° . Hence, the proposed design model can show a significant performance when being utilized in stealth applications which requires wide band operation, thereby overcoming the limitation of narrow band operation of patch antenna.

2.1. Design of Proposed Antenna

The patch (reference) antenna is designed to resonate at 8.4 GHz and coaxially fed at $x = 4.6$ mm, $y = 0$ mm. The dimension of the substrate is 64.25 mm \times 64.25 mm. The antenna is built on the lossy dielectric FR4 substrate with relative permittivity $\epsilon_r = 4.4$ and loss tangent of $\tan(\delta) = 0.02$, and the metal portions of the metamaterial are designed with copper having conductivity of $\sigma = 5.8 \times 10^7$ S/m and thickness of 0.035 mm. Dimensions of the patch are as shown in Table 1 and depicted in Fig. 1(c). The schematic top view of antenna is shown in Figs. 2(a) and (b), respectively.

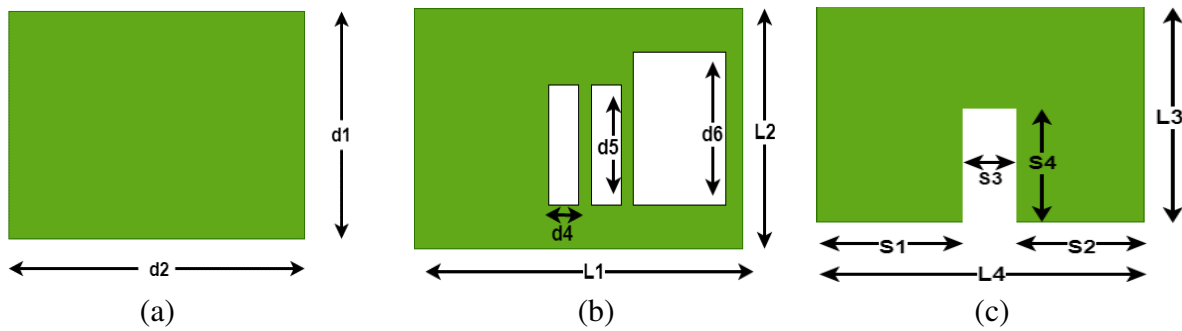


Figure 1. Schematic representation of (a) AMC1, (b) AMC2 and (c) slotted patch (reference antenna).

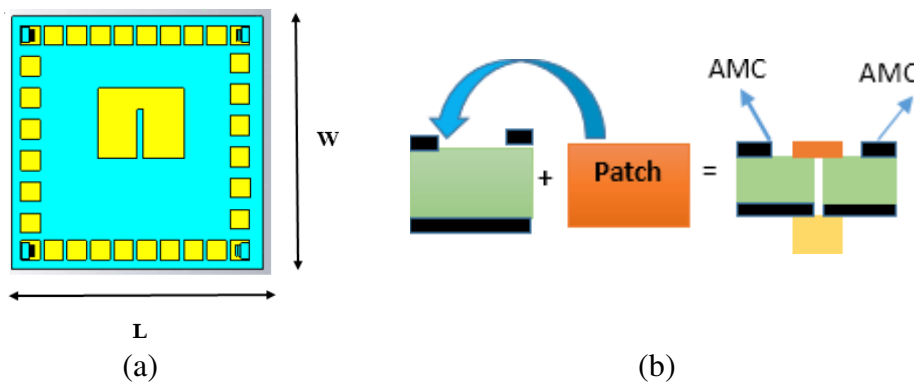


Figure 2. Configuration of low RCS MS antenna. (a) Top view, (b) side view of the antenna with coaxial feed.

Table 1. Parameters used in proposed antenna design.

Parameters	Value (mm)	Parameters	Value (mm)	Parameters	Value (mm)
d_1	5	d_3	2	s_1	10
d_2	5	d_4	0.4	s_2	10.5
L_1	5	d_5	2.7	s_3	1.5
L_2	5	d_6	3.5	s_4	12.5
L_3	22	L_4	18	-	-

2.2. Design of Proposed AMC Unit Cell

The proposed AMC1 has lengths of $d_1 = 5$ mm and $d_2 = 5$ mm, and AMC2 has lengths of $L_1 = 5$ mm, $L_2 = 5$ mm, $d_3 = 2$ mm, $d_4 = 0.4$ mm, $d_5 = 2.7$ mm, and $d_6 = 3.5$ mm as given Figs. 1(a) and (b). The dimensions of AMCs are as shown in Table 1. The array of unit cells AMC1 & AMC2 has been placed around the planar antenna, as shown in Fig. 2(a). The AMC's parameters are optimized to improve the antenna's performance. The unit cell and open boundary conditions are utilized to simulate the infinite unit cell structure using CSTMWS.

2.3. Design of Proposed Antenna Integrated with AMC

The patch antenna resonating at 8.4 GHz is arranged in the middle of the unit cells, and the side view of the antenna is shown in Fig. 2(b). The patch is coaxially fed, whose impedance is matched to 50Ω . The

reference (patch) antenna and AMC unit cell structure are constructed on an FR-4 substrate of 1.6 mm thickness. The overall dimension of antenna is $(L \times W)$ 64.25 mm \times 64.25 mm. The unit cell structure is employed to improve the antenna directivity. The microstrip patch is employed as a radiator [16].

3. SIMULATED RESULTS AND DISCUSSION

3.1. Theoretical Analysis of AMC Metasurface

Artificial Magnetic Conductors (AMCs) are the structures yielding high impedance at resonance, and they suppress the surface waves. The AMC design comprises a dielectric substrate sandwiched between the top and bottom metallic layers. These structures cancel out the backscattering waves from the antenna [27, 30]. The basis of AMC surfaces is such that wave's reflection energies are scattered and will cancel each other to form a divergent scattering pattern rather than the usual specular reflection. The RCS reduction concept of AMCs can be interpreted with a planar array with 180° phase reflections within a band of frequencies. Compared with a metallic board, the MS can significantly diminish RCS in specular directions. The ratio of the scattered field E_s to the incident field E_i can be expressed in terms of average reflection coefficient of the reflecting screen, when the plane wave illuminates normally to the AMC reflecting screen [27, 30].

$$\frac{E_s}{E_i} = \frac{A_1 e^{i\theta_1} + A_2 e^{i\theta_2}}{2} \quad (1)$$

where A_n and O_n ($n = 1, 2$) are the reflection amplitude and phase of AMC1 and AMC2, respectively. The RCS reduction more than 10 dB is required as compared to the perfect electric conductor (PEC) surface of the same size.

$$-10 \text{ dB} \geq 10 \log \frac{\lim_{r \rightarrow \infty} [4\pi r^2 |S|^2 / |I|^2]}{\lim_{r \rightarrow \infty} [4\pi r^2 (1)^2]} \quad (2)$$

By applying Eq. (1), the reflection phase difference can be calculated by

$$\left| e^{i\theta_1} + e^{i\theta_2} \right| = \sqrt{2(1 + \cos(\theta_1 - \theta_2))} \leq 0.6325 \quad (3)$$

$$143^\circ \leq |\Delta\varphi| = |\varphi_1 - \varphi_2| \leq 217^\circ \quad (4)$$

3.2. Scattering and Radiation and Performance of the Antenna

3.2.1. Reflection Phase of Reference, AMC Metasurface Antenna

The ultra-wideband RCS reduction has been acquired by the basis of phase cancellation. The reflection phase of metamaterial antenna and reference antenna varies from 160° to 140° , seen from Fig. 3. The multiple resonances at 4 GHz, 8 GHz, and 11.5 GHz approve the diffusive wave scattering leading to a desperate phase variation which accomplishes the phase cancellation. The reflection phase difference of AMC unit cells and reference patch antenna is shown in Fig. 3. From Fig. 3, it is evident that the proposed metasurface antenna demonstrates a reflection phase shift from $+180^\circ$ to -180° .

3.2.2. Reflection Coefficient of Antenna

The simulation results show that the size of the metallic patch affects return loss and thereby the impedance matching. Increasing the size of the metallic plate improves the return loss of the patch antenna with regular ground plane because the metallic plate directly acts as an extension of the original ground plane of the antenna.

The reference (patch) antenna has a reflection coefficient of -25 dB whereas the AMC loaded metasurface antenna has better impedance matching, and the depicted reflection coefficient is -28 dB at 8.4 GHz as observed from Fig. 4.

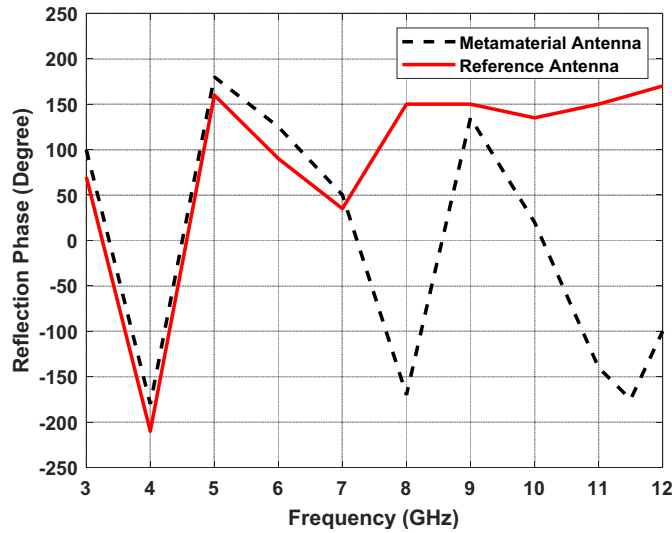


Figure 3. Reflection phase characteristics of metamaterial and reference antenna.

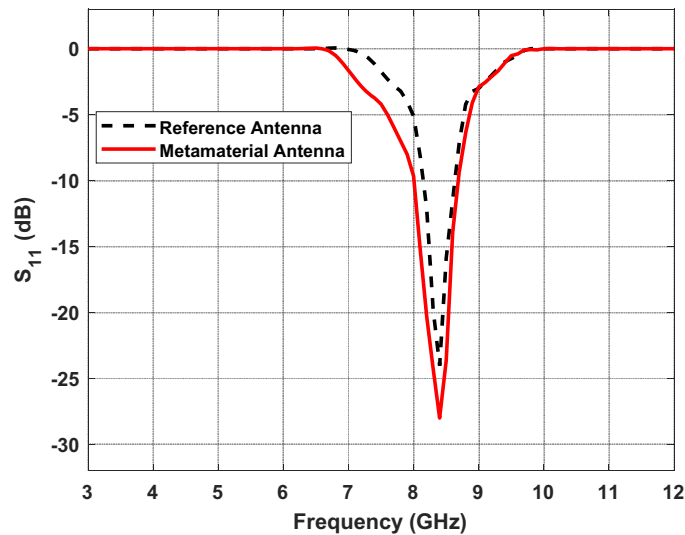


Figure 4. S_{11} parameter of metamaterial antenna and reference antenna.

3.2.3. Surface Current Distribution for the Proposed Antenna at Various Frequencies 5, 7.5, 11.5 GHz

The surface current distributions for the proposed antenna under x -polarized conditions were studied at various frequencies. At 5 GHz, we have noticed that the field currents are localized in the outer layer of the AMC unit cell and relatively smaller currents in patch antenna from Fig. 5(a). At 7.5 GHz, the field currents are concentrated on the middle patch antenna and also on surrounding AMC unit cells as noticed from Fig. 5(b). At 11.5 GHz, we notice that the fields are scattered more in the inner patch antenna, and the surroundings of metasurface antenna are seen from Fig. 5(c).

The radiation patterns of the antenna in the E -plane and H -plane are presented in Fig. 6(a). The radiation pattern of the antenna for the two planes are similar. The directivity defines the energy concentrated in a single direction rather than all the other directions. The energy scattering at the boresight direction assures that the directivity of the antenna is good. The size of the metallic plate also affects the radiation efficiency. Based on the simulations, the patch antenna with AMC unit cells has higher radiation efficiency than the regular patch antenna. This is due to the suppression of

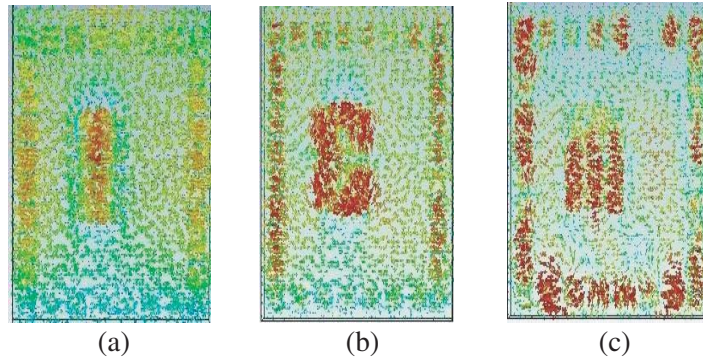
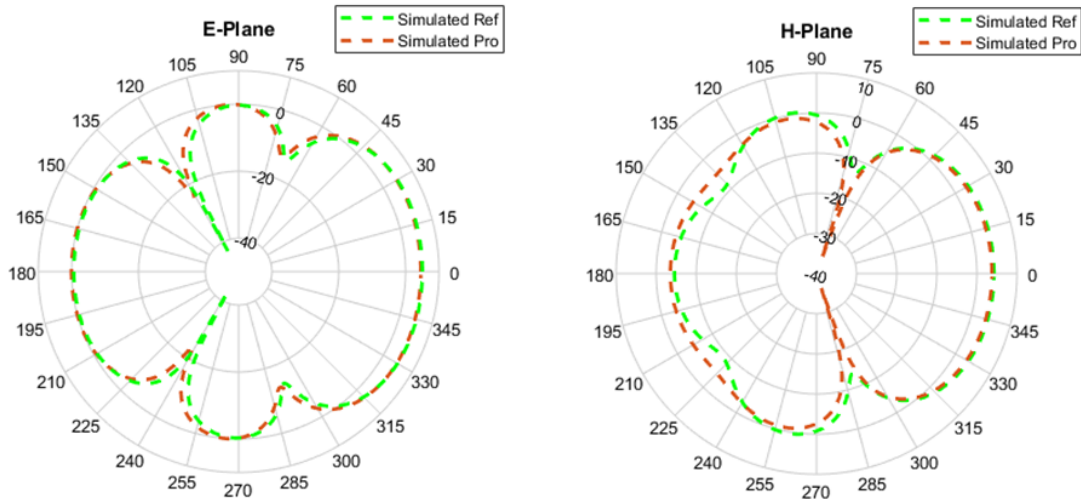
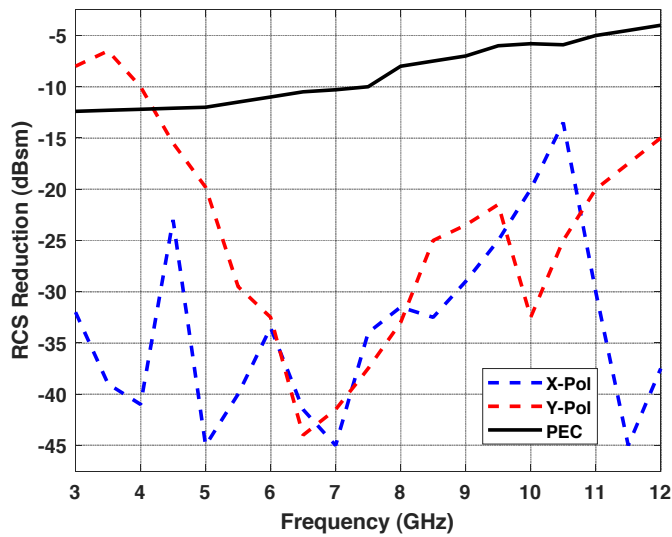


Figure 5. Surface current electric field dispersion of proposed antenna at distinct frequencies for x -polarized wave at (a) 5 GHz, (b) 7 GHz, (c) 11.5 GHz.



(a)



(b)

Figure 6. (a) E/H plane radiation pattern of proposed antenna at 8.4 GHz, (b) simulated RCS reduction under normal incidence.

surface waves gained by AMC surface. Generally, it is observed from the simulation results that the directivity increases when the patch antenna is attached to the AMC unit cells. However, the bigger plate remarkably changed the radiation pattern of the regular patch antenna.

The AMCs of the proposed antenna can diminish the in-band RCS considerably. To authenticate this simulated monostatic RCSs of the proposed antennas in x and y polarized modes are given in Fig. 6(b). The relation between PEC and RCS reduction is presented. It is shown that PEC has a slight effect on the RCS reduction. The 10 dB RCS reduction was achieved from 3–12 GHz (61.2%). In x -polarization the maximum RCSR of 45 dB occurs at 5, 7, and 11.5 GHz. In y -polarization 10 dB reduction band is from 4–12 GHz, and maximum reduction of 42 dB at 6.4 GHz has been observed.

4. FABRICATION AND EXPERIMENT RESULTS

To confirm the validity of the simulation, the prototypes of the proposed and reference antennas are fabricated and measured. Photographs of the proposed antenna top, bottom views are shown in Fig. 7. The Agilent Microwave analyzer N9917A is used to test the impedance characteristics of the two antennas. The measurement setup of the wave scattering of antenna is as shown in Fig. 8.

The S_{11} parameters of the simulated and measured results are shown in Fig. 9(a). From the plot, it is observed that the reflection coefficients of the simulated and fabricated antennas are relatively good. The measured and simulated radar cross section reduction (RCSR) values are compared and

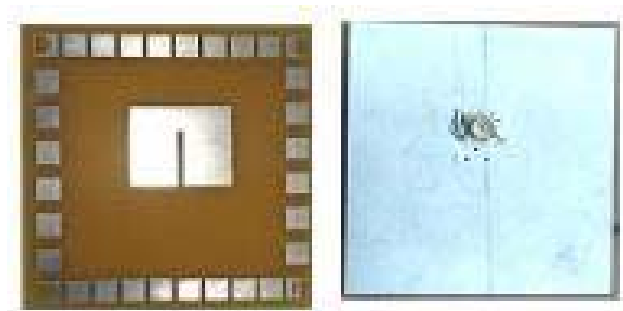


Figure 7. Fabricated prototype top and bottom view.

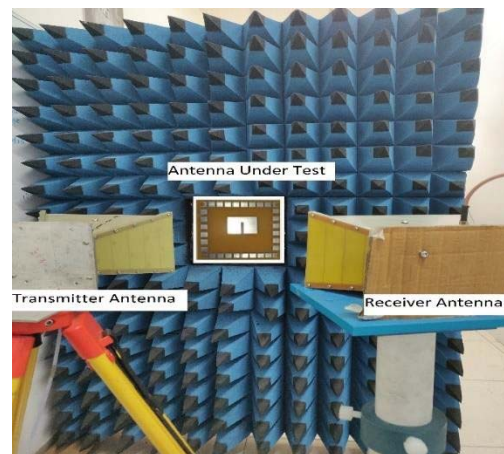


Figure 8. Measurement setup.

Table 2. Comparison of proposed antenna with antennas in literature.

Literature	Resonant frequency (GHz)	RCSR Bandwidth (GHz)	Size of the antenna	Max RCSR (dB)
[15]	3	6.2–12	$0.9\lambda \times 0.9\lambda$	24
[28]	10	9.2–14	$3.73\lambda \times 3.73\lambda$	20
[29]	7.8	4–12	$2.2\lambda \times 2.2\lambda$	11
[30]	6	5–12	$0.82\lambda \times 0.82\lambda$	15
[31]	5	8.5–12	$0.82\lambda \times 0.93\lambda$	24
[32]	11	6–12	$1.12\lambda \times 1.12\lambda$	17
[33]	6	2–12	$0.93\lambda \times 0.93\lambda$	15
Proposed antenna	8.4	3–12	$0.85\lambda \times 0.85\lambda$	45

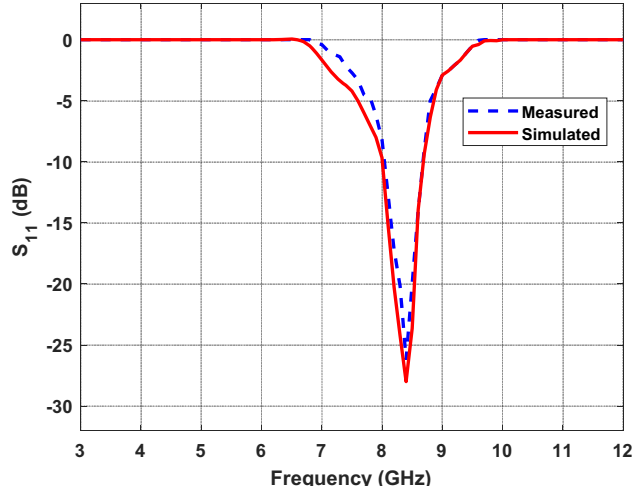
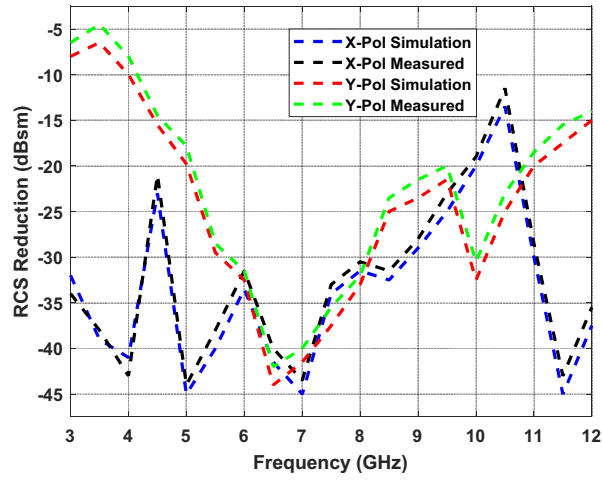
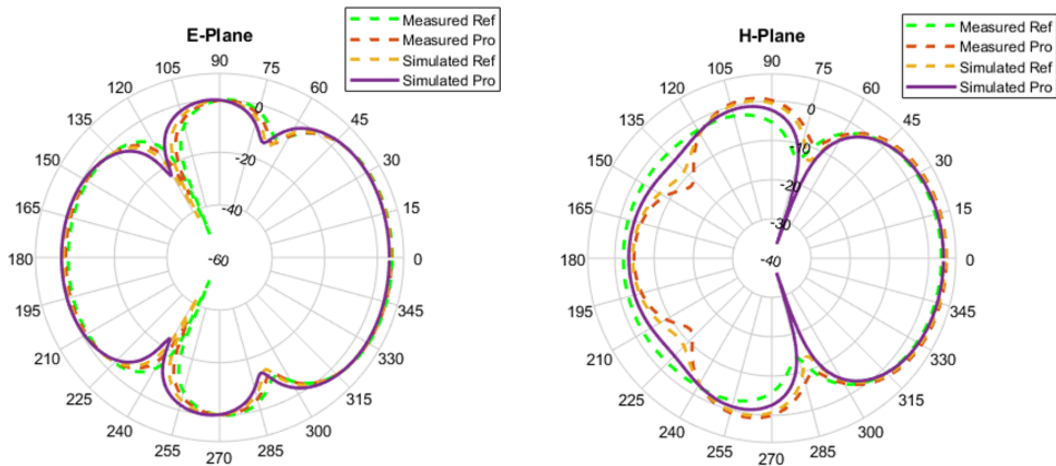


Figure 9. Reflection coefficient of MS antenna.



(a)



(b)

Figure 10. (a) Measured and simulated RCS reduction in x, y polarization, (b) measured and simulated radiation pattern in E -plane, H -plane at 8.4 GHz.

shown in Fig. 10(a). The measured RCS is realized as 43 dB at the three resonances 5 GHz, 7 GHz, 11.5 GHz for x -polarized wave. The in-band RCS reduction of the metasurface antenna is better than the reference antenna as observed from Fig. 10(a). From the above results, it has been observed that the simulation and measurement results are in good compliance, and a small deviation is due to fabrication and measurement tolerances.

The radiation performances of the metamaterial and reference antennas at 8.4 GHz are shown in Fig. 10(b). It can be seen that the radiation patterns of the measured and simulated antennas are in good agreement. There is a small deviation of 0.2 dB in measured gain compared to the simulated gain due to cable losses. The radiation patterns of proposed and reference antennas in E/H plane are similar. The radiation performance of the planar antenna was preserved good as we achieve a wide band RCSR. The metasurface antenna has more directional beam than the reference antenna ensuring that it has a better gain than the reference antenna in the boresight direction.

The proposed antenna is compared with the existing antennas in literature. The RCS reduction bandwidth of the proposed antenna is higher than the existing works. In addition, we have obtained the maximum RCSR of 45 dB which is larger than the other works. The size of the antenna is smaller than the existing antennas. From Table 2, it is evident that the proposed antenna is very effective in RCS reduction notably with smaller size.

5. CONCLUSION

In this paper, the RCS reduction of a patch antenna integrated with two disparate AMC unit cells has been presented. This novel design diminishes backscattering of EM waves thus minimizing the reflections from the target. The reflected waves scatter from the metasurface with a phase variation of $180^\circ \mp 30^\circ$ and cause a destructive interference in the frequency range of 3–12 GHz. A salient feature of the structure is that it requires less metal when being observed with the regular designs. Furthermore, by adding these AMCs, the antenna performance such as scattering, radiation has not been influenced. The proposed antenna proves to be better than the existing ones in terms of 10 dB RCS reduction and produces a wider bandwidth of 3–12 GHz (61.2%) with a peak RCSR of 45 dB. The measured results of the reflection coefficient and radiation pattern are in good agreement with simulation ones. The proposed compact, low profile antenna can be used for aircraft and stealth applications.

REFERENCES

1. Zhu, X., J. Gao, B. Zhu, J. Wang, Y. Tang, H. Yu, and S. Wang, "A low-RCS, wideband and circularly polarized metasurface antenna," *2018 IEEE MTT-S International Wireless Symposium (IWS)*, 1–3, IEEE, May 2018.
2. Liu, Y., K. Li, Y. Jia, Y. Hao, S. Gong, and Y. J. Guo, "Wideband RCS reduction of a slot array antenna using polarization conversion metasurfaces," *IEEE Transactions on Antennas and Propagation*, Vol. 64, No. 1, 326–331, 2015.
3. Knott, E. F., *Radar Cross Section Measurements*, Springer Science & Business Media, 2012.
4. Singh, H. and R. M. Jha, *Active Radar Cross-section Reduction*, Cambridge University Press, 2015.
5. Zhao, S.-C., B.-Z. Wang, and Q.-Q. He, "Broadband radar cross section reduction of a rectangular patch antenna," *Progress In Electromagnetics Research*, Vol. 79, 263–275, 2008.
6. Alibakhshi-Kenari, M., B. S. Virdee, L. Azpilicueta, M. Naser-Moghadasi, M. O. Akinsolu, C. H. See, and T. A. Denidni, "A comprehensive survey of metamaterial transmission-line based antennas: Design, challenges, and applications," *IEEE Access*, Vol. 8, 144778–144808, 2020.
7. Alibakhshi-Kenari, M., B. S. Virdee, P. Shukla, N. O. Parchin, L. Azpilicueta, C. H. See, and E. Limiti, "Metamaterial-inspired antenna array for application in microwave breast imaging systems for tumor detection," *IEEE Access*, Vol. 8, 174667–174678, 2020.
8. Alibakhshi-Kenari, M., "Design and modeling of new UWB metamaterial planar cavity antennas with shrinking of the physical size for modern transceivers," *International Journal of Antennas and Propagation*, 2013.

9. Alibakhshi-Kenari, M., B. S. Virdee, C. H. See, R. Abd-Alhameed, F. Falcone, and E. Limiti, "A novel 0.3–0.31 THz GaAs-based transceiver with on-chip slotted metamaterial antenna based on SIW technology," *2019 IEEE Asia-Pacific Microwave Conference (APMC)*, 69–71, IEEE, Dec. 2019.
10. Alibakhshi-Kenari, M., M. Khalily, B. S. Virdee, C. H. See, R. A. Abd-Alhameed, and E. Limiti, "Mutual-coupling isolation using embedded metamaterial EM bandgap decoupling slab for densely packed array antennas," *IEEE Access*, Vol. 7, 51827–51840, 2019.
11. Alibakhshi-Kenari, M., M. Naser-Moghadasi, R. A. Sadeghzadeh, B. S. Virdee, and E. Limiti, "Traveling-wave antenna based on metamaterial transmission line structure for use in multiple wireless communication applications," *AEU-International Journal of Electronics and Communications*, Vol. 70, No. 12, 1645–1650, 2016.
12. Alibakhshi-Kenari, M. and M. Naser-Moghadasi, "Novel UWB miniaturized integrated antenna based on CRLH metamaterial transmission lines," *AEU-International Journal of Electronics and Communications*, Vol. 69, No. 8, 1143–1149, 2015.
13. Alibakhshi-Kenari, M., B. S. Virdee, C. H. See, R. A. Abd-Alhameed, F. Falcone, and E. Limiti, "High-isolation leaky-wave array antenna based on CRLH-metamaterial implemented on SIW with $\pm 30^\circ$ frequency beam-scanning capability at millimetre-waves," *Electronics*, Vol. 8, No. 6, 642, 2019.
14. Jiang, W., Y. Liu, S. Gong, and T. Hong, "Application of bionics in antenna radar cross-section reduction," *IEEE Antennas and Wireless Propagation Letters*, Vol. 8, 1275–1278, Nov. 2009.
15. Pazokian, M., N. Komjani, and M. Karimipour, "Broadband RCS reduction of microstrip antenna using coding frequency selective surface," *IEEE Antennas and Wireless Propagation Letters*, Vol. 17, 1382–1385, Aug. 2018.
16. Jang, H. K., W. J. Lee, and C. G. Kim, "Design and fabrication of a microstrip patch antenna with a low radar cross section in the X-band," *Smart Materials and Structures*, Vol. 20, No. 1, 7–15, Dec. 2010.
17. Genovesi, S., F. Costa, and A. Monorchio, "Low-profile array with reduced radar cross section by using hybrid frequency selective surfaces," *IEEE Transactions on Antennas and Propagation*, Vol. 60, No. 5, 2327–2335, Mar. 2012.
18. Costa, F., S. Genovesi, and A. Monorchio, "A frequency selective absorbing ground plane for low-RCS microstrip antenna arrays," *Progress In Electromagnetics Research*, Vol. 126, 317–332, 2012.
19. Liu, Z., Y. Liu, and S. Gong, "Gain enhanced circularly polarized antenna with RCS reduction based on metasurface," *IEEE Access*, Vol. 6, 46856–46862, 2018.
20. Tan, Y., N. Yuan, Y. Yang, and Y. Fu, "Improved RCS and efficient waveguide slot antenna," *Electron. Lett.*, Vol. 47, No. 10, 582–583, May 2011.
21. Ravi, P. R., V. A. Libimol, K. K. Sreelatha, T. A. Nisamol, and C. K. Aanandan, "Low RCS microstrip patch antenna using complementary split-ring resonators," *IJIRSET*, Vol. 7, No. 6, 40–47, Mar. 2017.
22. Kong, X., J. Xu, J. J. Mo, and S. Liu, "Broadband and conformal metamaterial absorber," *Frontiers of Optoelectronics*, Vol. 10, No. 2, 124–131, Apr. 2017.
23. Jia, Y., Y. Liu, S.-X. Gong, T. Hong, and D. Yu, "Printed UWB end-fire Vivaldi antenna with low RCS," *Progress In Electromagnetics Research Letters*, Vol. 37, 11–20, 2013.
24. Yao, P., B. Zhang, and J. Duan, "A broadband artificial magnetic conductor reflecting screen and application in microstrip antenna for radar cross-section reduction," *IEEE Antennas and Wireless Propagation Letters*, Vol. 17, No. 3, 405–409, Mar. 2018.
25. Shater, A. and D. Zarifi, "Radar cross section reduction of microstrip antenna using dual-band metamaterial absorber," *Applied Computational Electromagnetics Society Journal*, Vol. 32, No. 2, 135–140, Feb. 2017.
26. Zhao, Y., X. Cao, J. Gao, X. Yao, T. Liu, W. Li, and S. Li, "Broadband low-RCS meta surface and its application on the antenna," *IEEE Transactions on Antennas and Propagation*, Vol. 64, No. 7, 2954–2962, Jul. 2016.

27. Modi, A. Y., C. A. Balanis, C. R. Birtcher, and H. N. Shaman, "The novel design of ultra-broadband radar cross section reduction surfaces using artificial magnetic conductors," *IEEE Transactions on Antennas and Propagation*, Vol. 65, No. 10, 5406–5417, Oct. 2017.
28. Tan, Y., J. Wang, Y. Li, J. Zhang, Y. Han, and S. Qu, "Low-RCS and high-gain circularly polarized metasurface antenna," *IEEE Transactions on Antennas and Propagation*, Vol. 67, No. 12, 7197–7203, 2019.
29. Nguyen-Trong, N., H. H. Tran, T. K. Nguyen, and A. M. Abbosh, "A compact wideband circular polarized Fabry-Perot antenna using resonance structure of thin dielectric slabs," *IEEE Access*, Vol. 6, 56333–56339, 2018.
30. Liu, Y., H. Wang, Y. Jia, and S.-X. Gong, "Broadband radar cross-section reduction for microstrip patch antenna based on hybrid AMC structures," *Progress In Electromagnetics Research C*, Vol. 50, 21–28, 2014.
31. Jang, H. K., W. J. Lee, and C. G. Kim, "Design and fabrication of a microstrip patch antenna with a low radar cross section in the X-band," *Smart Mater. Struct.*, Vol. 20, 1–8, Dec. 2010.
32. Yang, H.-H., X.-Y. Cao, Q.-R. Zheng, J.-J. Ma, and W.-Q. Li, "Broadband RCS reduction of microstrip patch antenna using bandstop frequency selective surface," *Radio Engineering*, Vol. 22, No. 4, 1275–1280, Dec. 2013.
33. Turpin, J. P., P. E. Sieber, and D. H. Werner, "Absorbing ground planes for reducing planar antenna radar cross-section based on frequency selective surfaces," *IEEE Antennas and Wireless Propagation Letters*, Vol. 12, 1456–1459, Nov. 2013.